

1

2 A ^{11}B and ^{31}P MAS NMR Study of the Impact of Ca^{2+}
3 and Sr^{2+} Network Modifying Cations on the Structure
4 of Borate and Borophosphate Glasses

5 *Tony Jin¹, Guy M. Bernard¹, Mark Miskolzie¹, Victor V. Terskikh²*
6 *and Vladimir K. Michaelis^{1*}*

7 *1- Department of Chemistry, University of Alberta, Edmonton, Alberta T6G 2G2, Canada*

8 *2- Department of Chemistry, University of Ottawa, Ottawa, Ontario K1N 6N5, Canada*

9

10

11

12 **Corresponding Author: Vladimir K. Michaelis, vladimir.michaelis@ualberta.ca*

13

14

15

16 **Keywords:** MAS NMR, disorder, medium-range structure, borate, borophosphate, ^{11}B , ^{31}P

17 **Abstract**

18 A detailed qualitative and quantitative analysis into the local- and medium-range order
19 of alkaline-earth binary borate and ternary borophosphate glasses is carried out through the
20 use of ^{11}B and ^{31}P magic-angle spinning nuclear magnetic resonance (MAS NMR) spectroscopy.
21 A series of calcium and strontium borate and borophosphate glasses were prepared with a
22 constant $\text{P}_2\text{O}_5:\text{B}_2\text{O}_3$ ratio of 0.4 and varying alkaline-earth loading contents in order to
23 understand the charge compensation characteristics of B and P within the glasses. For the
24 alkaline earth borate glass with loading values up to $R = 0.4$ (where R is the ratio between
25 alkaline earth metal oxide and borate moieties), the glass network preferentially forms
26 negatively-charged four-coordinate borate units to balance out the cationic charge of the
27 alkaline-earth network modifier. At higher alkaline-earth loading values of $R > 0.5$ there is a
28 mixture between three- and four-coordinate borate species balancing out the modifier. On the
29 other hand, investigation of the alkaline-earth borophosphate glass series indicates that these
30 compounds form a complex network with depolymerization of the phosphate species while
31 maintaining medium-range connectivity of the borate units within the amorphous solid. At
32 low alkaline-earth loadings, characteristics of BPO_4 , clustering is seen, while at high loading
33 values, negatively charged phosphate units are seen bridging to four-coordinate boron species
34 forming a complex mixed former oxide network. Ultrahigh-field ^{11}B MAS NMR helps to
35 determine the varying degrees of ring and non-ring borate species present within these
36 glasses, and confirms the unique structures present in both the binary borate and ternary
37 borophosphate series. The ^{31}P MAS NMR data suggests that calcium prefers a phosphate
38 chemical environment at high R , whereas strontium appears to maintain higher N_4 values over
39 the same composition range.

40 **1. Introduction**

41 Our interest in borophosphate glasses at the moment primarily focuses on the two
42 active components of B_2O_3 and P_2O_5 and their resulting effects on the glass structure-property
43 relationships. Phosphate-based multicomponent glasses are seen to have interesting chemical
44 and physical properties¹ such as lower dissolution rates² and optical properties,³ while the
45 addition of B_2O_3 is seen to markedly increase durability.⁴ The addition of other network-
46 modifying oxides such as alkali and alkaline-earth metals (i.e., Li, Na, K, Ca, Sr) extend their
47 potential use to other applications including nonlinear optical (NLO) materials,⁵ hermetic
48 sealing substances,⁶ and ion conductors.⁷ Additionally, the biocompatibility of these
49 compounds leads to their applications as biomaterials in the health and dental fields, since
50 calcium is a prominent ion in promoting hydroxyapatite formation and strontium is a
51 component in drug bases used in efforts to combat osteoporosis.^{8,9,10} However, principal
52 structural knowledge of low phosphate-containing borate glasses remains elusive, as the
53 addition of phosphate to boron oxide produces a mixed network-forming glass that lacks long-
54 range periodic order, and thus is very difficult to study under traditional X-ray diffraction
55 techniques. Moreover, the addition of alkaline-earth network modifiers impacts the local
56 structure of the glass, making irregular local environments too complex to observe by many
57 ordinary spectroscopic means.¹¹ Solid-state nuclear magnetic resonance (NMR) spectroscopy
58 on the other hand is one of the few characterization tools (e.g., X-ray absorption spectroscopy,
59 neutron diffraction, vibrational spectroscopy, etc.) capable of measuring the local and
60 medium-range structural units of these amorphous materials.^{12,14} ^{11}B and ^{31}P are highly
61 sensitive NMR-active nuclei due to their favorable gyromagnetic ratio and high natural
62 abundance. Hence, the far-reaching ability of ^{11}B and ^{31}P NMR spectroscopy can reveal
63 important correlations between atomic-level structures within a variety of glass networks.^{15,16}

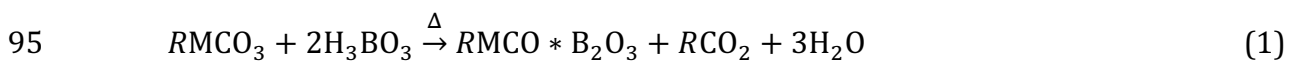
64 For example, the three- ($^{[3]B}$) and four-coordinate ($^{[4]B}$) boron chemical environments can be
65 clearly distinguished under ^{11}B magic-angle spinning (MAS) NMR with suitable magnetic field
66 strengths of 11.7 T or higher.¹⁷ Closer examination of the peaks ascribed to the $^{[4]B}$ region can
67 lead to an understanding of the medium-range structure as the ^{11}B isotropic chemical shift is
68 sensitive to phosphate neighbours, while ultrahigh magnetic fields and advanced NMR
69 techniques such as multiple-quantum magic-angle spinning (MQMAS) can lead to the
70 delineation of varying $^{[3]B}$ environments.^{18,19} NMR methods for the determination of medium-
71 range homonuclear and heteronuclear distances and connectivity has evolved over the last
72 two decades using various one- and two-dimensional techniques further assisting in
73 understanding glass structure.^{20, 21,22,23,24,25} ^{31}P MAS NMR offers additional insight into the
74 degree of depolymerization of the phosphate network such as the transformation from
75 bridging to non-bridging oxygens that may lead to the elucidation of neighbouring network
76 formers.²⁶ ^{43}Ca and ^{87}Sr are typically not studied due to their challenging NMR properties
77 including low natural abundance, low gyromagnetic ratio and moderately sized quadrupole
78 moments.^{27, 28, 29, 30} In addition to these problematic NMR properties, the structural
79 disordered and low concentration of network modifying cations leads to further complications
80 due to the limitations in sensitivity.

81 In this study, we examine the impact of altering the calcium and strontium ratios within
82 borate and borophosphate glasses on the network forming roles of borate and the impact
83 phosphate incorporation has on the local structure. Two series of calcium- and strontium-
84 modified glasses were examined while maintaining a constant $P_2O_5:B_2O_3$ ratio, K , where $K = 0$
85 or 0.4. These compositions provide a comparison on how P substitution affects glass
86 polymerization as the concentration of network modifying cations (Ca or Sr) is varied. Results
87 from ultrahigh-field ^{11}B MAS NMR (21.1 T) also provide clear evidence of distinct $^{[3]B}$ ring

88 formation within high alkaline-earth borophosphates, a feature not observed for alkaline-
89 earth borate glasses with comparable alkaline-earth modifier concentrations.

90 **2. Materials and Methods**

91 2.1 Synthesis: Binary alkaline-earth borate and ternary alkaline-earth borophosphate glasses
92 were prepared from reagent-grade (>98% pure) calcium or strontium carbonate, boric acid,
93 and phosphorus pentoxide obtained from Sigma Aldrich. The following chemical reactions
94 describe the preparation of the binary and ternary glasses respectively:



97 where M is either calcium or strontium, R is the alkaline-earth oxide to boron trioxide molar
98 ratio ($R = \text{MO}/\text{B}_2\text{O}_3$) and K is the phosphorous pentoxide to boron trioxide molar ratio ($K =$
99 $\text{P}_2\text{O}_5/\text{B}_2\text{O}_3$). The glass samples were synthesized in 500 mg batches (to bypass the onset of
100 crystallization) by combining the proper ratios of alkaline-earth carbonate, boric acid, and
101 phosphorus pentoxide in a platinum(95%)/gold(5%) crucible (Laval Labs, Quebec, Canada).
102 The starting materials were kept in an oven set to 110 °C prior to weighing out the reactants;
103 once combined the crucible was pre-treated at 600-700 °C for 15 minutes to ensure
104 decarbonation was complete, and once the mass loss was confirmed the crucible was placed
105 into a preheated high-temperature box furnace (Carbolite Gero Ltd., Hope Valley, UK) between
106 1200 and 1300 °C for 1 to 2 hours. All final glasses were within $\leq 3\%$ of the expected final
107 masses. The melts were rapidly quenched to room temperature by dipping the crucible in
108 cooled deionized water. All glasses were characterized based on their translucent nature, as
109 well as with powder X-ray diffraction (XRD) to ensure that no crystallinity was present. Note:
110 Only the parent 0.4 $\text{P}_2\text{O}_5:\text{B}_2\text{O}_3$ glass, identified as BPO_4 , displayed considerable crystallinity,

111 with minor impurities observed in the R=0.05 calcium and strontium borophosphate samples.
112 Glass samples were packed into glass vials sealed with Parafilm and stored under dry
113 atmosphere in a dessicator.

114 2.2 Powder X-ray diffraction: The glasses were ground into a fine white powder in an agate
115 mortar and pestle before being mounted on a single crystal quartz (SiO₂) background sample
116 holder and analyzed using a Bruker PLATFORM diffractometer, CCD detector, Mo K_α source.
117 All data were acquired at room temperature with a 2θ range of 5° - 80° and 0.029° increments.

118 2.3 Solid-state nuclear magnetic resonance spectroscopy: ¹¹B and ³¹P NMR spectra were
119 acquired on an Agilent/Varian VNMRS 600 MHz spectrometer equipped with an Oxford
120 magnet ($B_0 = 14.1$ T). All spectra were acquired using a 3.2 mm triple resonance Varian MAS
121 probe. Powdered samples were placed into ZrO₂ rotors (3.2 mm o.d., 22 μL, 30 to 40 mg)
122 equipped with Torlon drive and top caps. All data were acquired using a spinning frequency of
123 16 kHz. ¹¹B NMR experiments used a short 0.4 μs Bloch excitation pulse (9° tip angle, $\gamma B_1/2\pi$
124 = 62.5 kHz), 4 s recycle delay, 16 dummy scans and 512 co-added transients. All spectra were
125 referenced using boric acid (H₃BO_{3(aq)}, 0.1 M) as a secondary reference, set to +19.6 ppm
126 (BF₃Et₂O, $\delta_{\text{iso}} = 0$ ppm). ³¹P NMR experiments were acquired using a Bloch pulse set to 1.6 μs
127 (45° tip angle, $\gamma B_1/2\pi = 71$ kHz), 120 s recycle delays, 4 dummy scans and 64 co-added
128 transients. Phosphoric acid (H₃PO_{4(aq)}, 85%) was used as a primary reference, set to 0.0 ppm.
129 Recycle delays were checked for each glass series to ensure quantification.

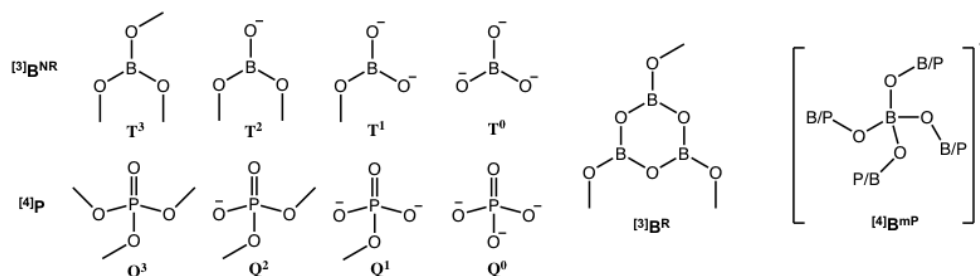
130 Ultrahigh field ¹¹B NMR spectra ($\nu_L = 288.6$ MHz) were acquired on a Bruker Avance II
131 900 (21.1 T) spectrometer at the Canadian National Ultrahigh-Field NMR Facility for Solids
132 (Ottawa, Canada). ¹¹B MAS NMR spectra were acquired on selected samples using a home-
133 built 2.5 mm double resonance boron-free MAS NMR probe with a spinning frequency of 20

134 kHz. Single pulse (Bloch) experiments used a short $0.4 \mu\text{s}$ pulse (9° tip angle, $\gamma B_1/2\pi = 62.5$
135 kHz), 5 s recycle delays, 4 dummy scans and 512 co-added transients. 3QMAS spectra were
136 acquired using a three-pulse MQMAS experiment with a zero quantum filter and a $\pi/2$
137 selective pulse ($\gamma B_1/2\pi = 62.5$ kHz, where p1 and p2 were optimized for maximum
138 sensitivity).^{31,32} All 3QMAS NMR experiments were acquired under identical conditions using
139 a 6 s recycle delay, 48 scans and 256 t_1 increments with an increment of $12.5 \mu\text{s}$ (4 rotor
140 periods). Spectra were referenced to 0.1 M boric acid (19.6 ppm, with respect to $\text{BF}_3\text{Et}_2\text{O}$, δ_{iso}
141 = 0 ppm). All spectra were processed using either TopSpin 3.5b (Bruker), VnmrJ4.2a (Agilent)
142 or SpinWorks 4.2 (K. Marat, UManitoba) software packages. MQMAS spectra were processed
143 using the shearing function as implemented within TopSpin. Exponential line broadening
144 between 10 and 50 Hz was applied to all spectra. ^{11}B MAS NMR spectra were simulated using
145 the STARS³³ software within VnmrJ to determine the quadrupolar coupling constants,
146 isotropic chemical shifts and to deconvolute the $^{[3]}\text{B}^{\text{R}}$ and $^{[3]}\text{B}^{\text{NR}}$ chemical environments. The
147 N_4 values were determined by peak integration of the 14.1 T data and corrected following the
148 Massiot et al.³⁴ method. Correction factors of 0.96 $^{[3]}\text{B}$ and 1.07 ($^{[4]}\text{B}$) were used based on our
149 ^{11}B MAS NMR experimental methods and determined quadrupole coupling parameters by
150 examining the central and satellite transitions of the borate and borophosphate glasses.

151

152 **3. Results and Discussion**

153 3.1 Boron and Phosphorus Speciation: The local speciation within borates and phosphates can
154 be made up from short- and medium-range structural units.^{13,14,35} To highlight these
155 structural changes caused by alkaline-earth network modifiers, the short-range structure is
156 defined by the oxide coordination environment and how that network is made up of either
157 bridging or non-bridging oxygens. Borate short-range units may be ^{[3]B} in a trigonal planar
158 structure comprised of zero non-bridging oxygens (T³) to all non-bridging oxygens (T⁰). It can
159 also be in the form of ^{[4]B} units, whereby a negative charge is delocalized over the whole
160 structural unit in a pseudo-tetrahedral chemical environment. Phosphorus atoms are four-
161 coordinate (^{[4]P}) quaternary units defined as Qⁿ units, where n defines the number of bridging
162 oxygens, from three for all bridging oxygens (Q³, [O=PO₃]⁰) to zero for three non-bridging
163 oxygens (Q⁰, [O=PO₃]³⁻). Medium-range structural information can also be obtained by careful
164 assessment of NMR line shapes and isotropic chemical shifts, including an ability to identify
165 borate rings (^{[3]B^R}) or non-ring (^{[3]B^{NR}}) units, and bridging boron-phosphorus neighbours to
166 four-coordinate boron environments, ^{[4]B^{mP}}, where m denotes the number of bridging
167 phosphate neighbours ranging from zero (all bridging borate neighbours, ^{[4]B^{0P}}) to four (all
168 bridging phosphate neighbours, ^{[4]B^{4P}}). Scheme 1 summarizes the structural units discussed
169 here.

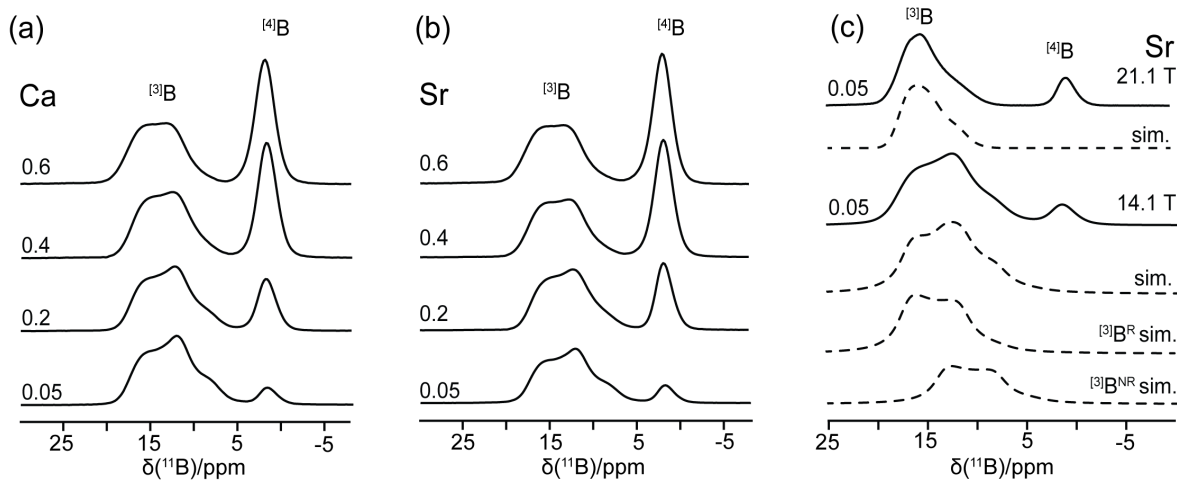


170

171 **Scheme 1: Short- and Medium-Range Structural Units in Borates and Phosphates**

172 3.2 Binary Borates: The $K = 0$ series of calcium and strontium alkaline-earth borate glasses
173 were first measured with ^{11}B MAS NMR to deduce the fraction of four-coordinate boron (N_4).
174 Figure 1 reveals resolution of two main boron environments at 14.1 T, the higher frequency
175 resonance (5 to 20 ppm) is assigned to $^{[3]}\text{B}$ with a characteristic quadrupolar coupling
176 constant, $C_Q = 2.5$ to 2.7 MHz, typically observed in borates.^{36,37} The unique lineshape features
177 for $R \leq 0.2$ are associated to $^{[3]}\text{B}^{\text{R}}$ and $^{[3]}\text{B}^{\text{NR}}$ borate units.³⁸ The ultrahigh-field ^{11}B MAS NMR of
178 the three-coordinate boron provides greater resolution of this region as the contribution to
179 the spectrum from the second-order quadrupole broadening scales inversely with magnetic
180 field strength, providing improved clarity to this region.³⁸ Figure 1c reveals contributions
181 from two ^{11}B resonances where the $^{[3]}\text{B}^{\text{R}}$ and $^{[3]}\text{B}^{\text{NR}}$ have isotropic chemical shifts of $\delta_{\text{iso}} = 18.0$
182 ± 0.5 and 14.5 ± 0.5 , respectively. The lower frequency four-coordinate resonance (5 to -5
183 ppm) is much narrower due to its higher symmetry pseudo-tetrahedral chemical environment
184 ($C_Q \approx 250$ to 500 kHz) with evidence of only a single BO_4 species.^{12,14,38} Evaluating these
185 spectra, the overall N_4 value with respect to R can be evaluated by peak integration of the 14.1
186 T data, where differences in the quadrupole coupling constants were corrected following the
187 method described in detail by Massiot et al.³⁹ As seen in Figure 2 there is an approximately
188 linear relationship for the plot of N_4 vs R both the calcium and strontium borate series, typical
189 behaviour among other borate glasses with cationic modifiers,^{14,40,42} in which the equation that
190 $N_4 = R$ holds up until $R = 0.5$ (correlation coefficients of 0.96 and 0.97 for CaB and SrB,
191 respectively). This effect is commonly observed in borates as the $^{[3]}\text{B}$ will convert to $^{[4]}\text{B}$
192 carrying a negative charge to compensate for the excess positive charge introduced through
193 the modifying Ca^{2+} or Sr^{2+} cations. Up to this point, the charge compensation mechanism of
194 the calcium and strontium borate glass has been the formation of BO_4^- units, which balances
195 out the positive cationic alkaline-earth network modifiers. Above an alkaline-earth loading of

196 about $R = 0.5$, a negative deviation occurs such that the excess charge from the cationic input is
197 compensated not only by the $^{[4]}B$ site, but also by the formation of non-bridging oxygens
198 (NBOs) in the local structure of the glass, in the form of T^2 units, as shown in Scheme 1. The
199 ratio of $^{[4]}B$ units and T^2 $^{[3]}B$ units can be obtained from a charge balance calculation such that
200 they balance the cationic charge. Using a sample case of $R = 0.5$ in the strontium borate series,
201 with an N_4 value of 0.44, there is still a fraction of 0.06 excess cationic charge left within the
202 system, which must be balanced, requiring the creation of negatively charged T^2 units with
203 anionic non-bridging oxygens.^{14,43} Thus the overall fraction of local units in the structure can
204 be calculated by means of the N_4 value, with 44% being the $^{[4]}B$ unit, 6% from the T^2 three-
205 coordinate site, and 50% based on the neutral trigonal T^3 units. Indeed, a careful analysis
206 reveals that increasing the R value further to a value of 0.6 leads to a steeper negative
207 deviation from the linear N_4 relationship, indicating increasing preference towards forming
208 NBOs in the form of T^2 units to charge balance rather than the BO_4^- four coordinate site as the
209 alkaline-earth loading is increased. This driving force in forming T^2 units above $R = 0.5$ is often
210 attributed to the avoidance of $^{[4]}B-O-^{[4]}B$ whereby it is energetically unfavorable to have two
211 negatively charged anions bridged by the same oxygen.⁴² Both the Ca^{2+} and Sr^{2+} samples
212 exhibit similar behaviour over the whole compositional range as the modifying concentration
213 increases above $R=0.5$, the N_4 fraction decreases as it begins to depolymerize forming NBOs (<
214 15%, based on charge balance arguments).

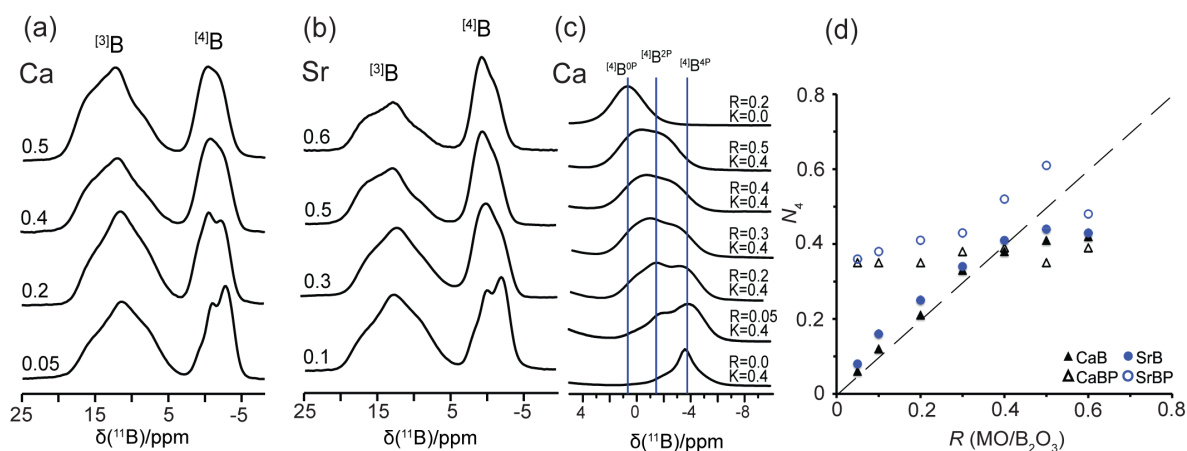


215

216 **Figure 1: ^{11}B MAS NMR spectra of (a) calcium and (b) strontium borates. (c) Strontium borate, $R=0.05$**
 217 **glass revealing the ring and non-ring contributions of the $^{[3]}\text{B}$ region at 14.1 and 21.1 T. Simulations**
 218 **are shown as dashed lines.**

219

220 3.3 Ternary Borophosphates: The calcium and strontium $K = 0.4$ borophosphate glass series
 221 (CaBP and SrBP) were also analyzed using ^{11}B MAS NMR spectroscopy to identify the fraction
 222 of four-coordinate boron. Figure 2 compares the borophosphate ($K = 0.4$) glass series over the
 223 same compositional range of Ca and Sr modifier ($R = 0.05$ to 0.6). As discussed above, both $^{[3]}\text{B}$
 224 and $^{[4]}\text{B}$ are present, with the N_4 increasing as the Ca or Sr modifier is added. What is unique
 225 about the ^{11}B NMR spectra is their remarkable sensitivity to the medium-range glass structure,
 226 markedly changing with the addition of network forming P_2O_5 as seen in alkali and alkaline-
 227 earth borophosphates.⁴⁴ Notably, at higher alkaline-earth loading, the ring contributions in
 228 the $^{[3]}\text{B}$ region of the borophosphate spectra remain high whereas those for the borates
 229 quickly lose this feature above $R = 0.2$, which is shown in Figure 3. This effect has been
 230 observed in other ternary composition glasses such as borosilicates whereby the
 231 depolymerization of the silicate units into non-bridging oxygens occurs to some extent,
 232 accommodating the excess charge prior to the formation of T^2 borate units.³⁸



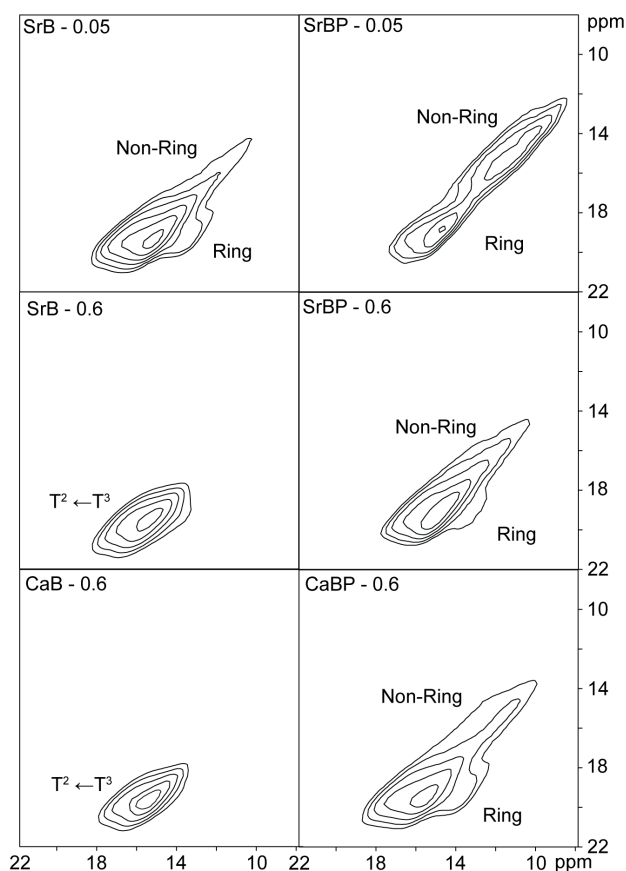
234

235 **Figure 2: ^{11}B MAS NMR spectra (11.7 T) of (a) calcium borophosphates and (b) strontium**
 236 **borophosphates with $K = 0.4$ and varying R values. (c) Ultrahigh-field (21.1 T) spectra comparing the**
 237 **$^{[4]}\text{B}$ regions of binary calcium borate ($K = 0$) to calcium borophosphates with varying K and R values.**
 238 **(d) Plot of N_4 vs R for all binary and ternary alkaline-earth borates and borophosphate glasses**
 239 **(dashed line is a guide set to 1:1).**

240

241 There are multiple overlapping $^{[4]}\text{B}$ resonances for the borophosphate series,
 242 representing various degrees of phosphate connectivity in the glass network, in contrast to the
 243 single peak observed for the corresponding spectra of the Ca and Sr borate glass series. As
 244 seen in Figure 2, the ^{11}B MAS NMR spectra indicate that there are two to three different $^{[4]}\text{B}$
 245 environments with varying degrees of P neighbours, as seen in other borophosphate glass
 246 series.¹⁷ The peaks shift to higher frequency with higher alkaline-earth content, indicating a
 247 change in the medium-range structure from $^{[4]}\text{B}$ rich with P neighbours converting to a $^{[4]}\text{B}$
 248 with B neighbouring environments. From past borophosphate studies utilizing crystalline
 249 models, quantum chemical calculations and dipolar recoupling approaches, the ^{11}B site with δ
 250 $\text{iso} \approx 1$ ppm is due to $^{[4]}\text{B}^{\text{OP}}$ while the peak to lowest frequency ($\delta_{\text{iso}} \approx -3.5$ ppm) is due to $^{[4]}\text{B}^{4\text{P}}$

251 with each P substitution for a B neighbour shifting the data to higher frequency by ~0.7
252 ppm.^{17,38}



253

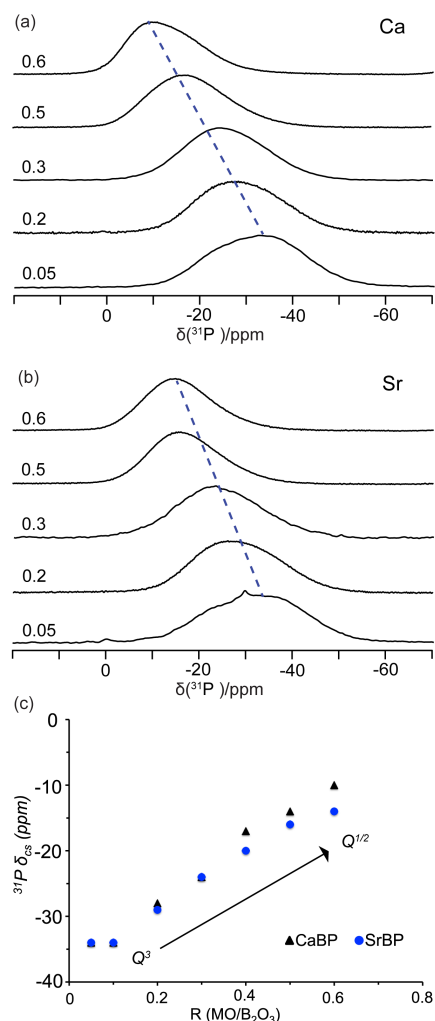
254 **Figure 3: ^{11}B 3QMAS NMR spectra ($B_0 = 21.1$ T) of the $^{[3]}\text{B}$ region showing the presence of ring and**
255 **non-ring contributions for selected calcium or strontium containing borate ($K = 0$, left hand side) and**
256 **borophosphate ($K = 0.4$, right hand side) glasses. Contour base levels were set to 10% of maximum**
257 **intensity and incremented by a factor of 1.45.**

258

259 Closer examination of the fraction of four-coordinate boron (Figure 2d) shows a large
260 positive deviation from the $N_4 = R$ relationship as seen in the $K = 0$ series. The glass structure
261 changes markedly with the addition of phosphates to the network, as this gives another
262 avenue by which the cationic alkaline-earth modifiers can be charge compensated. Notably, at
263 lower alkaline-earth loading, a positive deviation from the supposed $N_4 = R$ relationship

264 suggests drastic medium-order structural changes. As charge compensation requires, this
265 excess of anionic charge coming from the $^{[4]B}$ sites can only be balanced by the formation of a
266 positively charged local unit by the phosphate, PO_4^+ (Q^4), as is apparent from the crystalline
267 BPO_4 .^{17,45,46} X-ray diffraction and NMR spectroscopy of $K = 0.4$ and $R = 0$ (data not shown)
268 reveal the presence of amorphous and crystalline BPO_4 analogues, with $\delta_{iso}(^{11}B) = -3.3$ and
269 $\delta_{iso}(^{31}P) = -30$ ppm.^{47,48}

270 ^{31}P NMR spectroscopy provides information on the phosphate chemical environment,
271 in particular aiding in the assessment of the depolymerization of chains with alkaline-earth
272 loading. In the ^{31}P MAS NMR spectra for the calcium and strontium borophosphate series
273 shown in Figure 4, there is a remarkable change in the centre-of-gravity shift (δ_{cgs}) of the ^{31}P
274 MAS NMR resonance indicating a breakdown of the bridging oxygens within the phosphate
275 linkages. Previous ^{31}P NMR studies of phosphate glasses and crystals have shown that the
276 isotropic chemical shift generally trends to increase as quaternary phosphate units
277 depolymerize from bridging oxygens (Q^3) to orthophosphate, non-bridging units (Q^0).⁴⁹ As
278 seen from the ^{31}P NMR spectra of the higher R -value glasses (Figure 4), there is almost no
279 overlap of the peak from the Q^3 region (-30 ppm), and in fact Ca and Sr strongly favour Q^2
280 and/or Q^1 units. The N_4 values also agree with this, as between an R value of 0.5 and 0.6, there
281 is a crossover from positive deviation about the linear relationship $N_4 = R$ to a negative one.
282 This result indicates a change in the charge balancing behaviour in these glasses whereby the
283 positive cationic charge is being compensated by delocalized negatively charge $^{[4]B}$ units and
284 localized negatively charged NBOs located on Q^2 and Q^1 phosphate units.



285

286 **Figure 4:** ^{31}P MAS NMR spectra ($B_0 = 14.1$ T) of Ca (a) and Sr (b) borophosphate glasses ($K = 0.4$) with
 287 varying R values. Change in the peak maxima of the chemical shift (ppm) as a function of calcium and
 288 strontium network modifiers. The dashed lines are a guide for the eye, highlighting the shift in the
 289 centre of gravity. The $R = 0.05$ SrBP glass has a small crystalline impurity $<2\%$ (30 ppm).

290

291 Examination of the $\delta_{\text{cgs}}(^{31}\text{P})$ values for the strontium-containing $K = 0.4$ series (Figure
 292 4) shows an increase in chemical shift, indicating the conversion of fully bridging Q^3 (-30 to
 293 -50 ppm) units to depolymerized Q^2 (~ -20 ppm) units with a single non-bridging oxygen.
 294 Combining these observations with the ^{11}B MAS NMR results, there are clear B-O-P units
 295 present with the $^{[4]}\text{B}$ environments, indicating that the neighbouring P species are Q^2 linkages
 296 on the borate pseudo-tetrahedra. The calcium borophosphate glasses show similar behaviour

297 where the formation of non-bridging oxygens occur as Ca loading increases; however the
298 fraction of four-coordinate boron does not change as drastically over the compositional series,
299 while the ^{31}P NMR peaks shift quickly to the Q^1 (~ -10 ppm) region (Figure 4). Although, other
300 explanations are not excluded, we propose that this observation indicates that the Ca^{2+} cations
301 prefer a phosphate chemical environment, thus preferentially interact with the phosphate
302 rather than the borate units, whereas Sr^{2+} does not appear to exhibit this preference as
303 strongly, maintaining higher N_4 values over the same composition range (Figure 2d). This
304 behaviour may be related to the preferential stabilization of charge by NBOs rather than the
305 shared negative charge from $^{[4]}\text{B}$, similar to the behaviour of binary borate glasses.^{14,21} Other
306 possibilities include that the glass-forming ability improves with Sr, although crystalline
307 features in CaBP were not observed in the XRD analysis. The cation field strength (Sr: 0.29 vs.
308 Ca: 0.36) may be important in directing the physical properties within glassy materials,
309 however understanding the property-structure relationship and the impact that field strength
310 may have on direct atomic-level structure (e.g., coordination number, connectivity, etc.) is
311 beyond the scope of the current work, requiring carefully executed systematic studies.⁵⁰ What
312 is clear from this data is that Ca prefers NBO environments isolated on PO_4 units over the
313 delocalized negative charge on $^{[4]}\text{B}$ or localized negative charges found on T^1 or T^2 units. The
314 ^{11}B 3QMAS NMR spectra clearly indicate the presence of borate ring structures even at $R = 0.6$
315 Ca or Sr loadings (Figure 3). These findings suggest that the $^{[3]}\text{B}$ site medium-range structure
316 has a significant amount of ring component within these high R alkaline-earth borophosphate
317 glasses, while the $Q^{1/2}$ phosphate species interact with the tetrahedral borate units to some
318 extent due to the presence of $^{[4]}\text{B}^{2\text{P}}$ and $^{[4]}\text{B}^{1\text{P}}$ spectral signatures, *vide supra*.

319 **4. Conclusion**

320 We have focused on the role of alkaline-earth modifiers and their structural
321 implications on a series of binary borate and ternary borophosphate glasses, with emphasis on
322 short- and medium-range structure. The binary calcium and strontium borate series behave
323 similarly to other borate glasses with cationic loading, with a preference for forming T^2 units
324 at alkaline-earth loadings of more than $R = 0.5$. The aim of this study was to determine the
325 structural differences associated with the use of calcium and strontium oxide modifiers in
326 borophosphate glasses. The calcium cation clearly prefers a phosphate environment for
327 charge compensation, as the N_4 value is markedly lower than that of strontium. This
328 observation is also seen in the stark contrast in the peak positions seen in the ^{31}P MAS NMR
329 spectra, as the changes in δ_{cgs} with each R -value is seen to be much higher, with a resonance
330 within the Q^1 region for the calcium borophosphate glass $R = 0.6$ than for the strontium series.
331 This behaviour may be related to the preferential stabilization of charge by NBOs rather than
332 the shared negative charge from $^{[4]}\text{B}$. The presence of two very distinct medium-range
333 structural units at two primary alkaline-earth loading environments indicates a complexity
334 among the glass forming network that goes beyond the scope of the first coordination sphere.
335 It is apparent that any potential application of borophosphate glasses should be crucially
336 linked to a careful selection of the composition of the glass; a combination of ^{11}B and ^{31}P MAS
337 NMR spectroscopy provides a clear insight into the structure and thus will continue to play a
338 critical role in the advancement of these materials.

339 **Acknowledgements**

340 The Natural Sciences and Engineering Research Council (NSERC) of Canada Discovery Grant
341 Program and the University of Alberta are acknowledged for generous support of this

342 research. T.J. was partially supported through the University of Alberta Research Internship
343 (URI) program. The Association of Commonwealth Universities Early Career Academic Grant
344 supported a portion of this work. The authors thank Mr. Abishek Iyer, Dr. Wenlong Yin and Dr.
345 Arthur Mar for access to their XRD facility. Access to the 21.1 T NMR spectrometer was
346 provided by the National Ultrahigh-Field NMR Facility for Solids (Ottawa, Canada), a national
347 research facility funded by a consortium of Canadian Universities and by an NSERC RTI grant,
348 the National Research Council of Canada and Bruker BioSpin, and managed by the University
349 of Ottawa (<http://nmr900.ca>). V.K.M. thanks Dr. Jonathan Schaeffer, Dean of Science, Dr. Lorne
350 Babiuk, VP Research (University of Alberta), and the Deans and VPs of several other Canadian
351 universities for supporting the National Ultrahigh- Field NMR Facility for Solids.
352

-
- ¹ Youssef, N. H., Belkhiria, M.S., Videau, J. J. and Amara M. B. *Mater. Lett.*, 2000, 44, p. 269-274.
- ² Oelkers, E.H. and Montel, J.M. *Elements*, 2008, 4 (2), p. 113-116.
- ³ Hammi, M. and Maarooft, A. *Mater. Lett.*, 2016, 182, p. 227-230.
- ⁴ Frieser, R.G. in: *Electrocomponent Science and Technology Vol. 2* Gordon & Breach, New York, 1975, p. 163.
- ⁵ Boiteux, S.L., Segonds, P., Canioni, L., Sarger, L. *J. Appl. Phys.*, 1997, 81, p. 1481-1487
- ⁶ Wilder, J.A. *J. Non-cryst. Solids*, 1980, 38, p. 879
- ⁷ Storek, M., Adjei-Acheamfour, M., Christensen, R., Martin, S.W., Böhmer, R. *J. Phys. Chem. B*, 2016, 120 (19), p. 4482-4495
- ⁸ Cui, X., Huang, C., Zhang, M., Ruan, C., Peng, S., Li, L., Liu, W., Wang, T., Li, B., Huang, W., Rahaman M.N., Lu W.W., Pan, H., *J. R. Soc. Interface*, 2017, 14, 20161057
- ⁹ Liang, W., Tu, Y., Zhou, H., Liu, C., Rüssel, C., *J. Non-Cryst. Solids*, 2011, 357, p. 958-962
- ¹⁰ Massera, J., Shpotyuk, Y., Sabatier, F., Jouan, T., Boussard-Pledel C., Roiland, C., Bureau, B., Petit, L., Boetti, N. G., Milanese, D., Hupa, L., *J. Non-Cryst. Solids*, 2015, 425, p. 52-60
- ¹¹ Larink, D., Eckert, H., Reichart, M., Martin, S.W. *J. Phys. Chem. C*, 2012, 116 (50), p. 26162-26176
- ¹² P.J. Bray, *Inorg. Chim. Acta* 289 (1999) 158
- ¹³ W. Müller-Warmuth, H. Eckert, *Phys. Rep.* 88 (1982) 91.
- ¹⁴ Michaelis V.K., Aguiar, P. M., Kroeker, S. *J. Non-cryst. Solids*, 2007, 353, p. 2582-2590
- ¹⁵ Zielniok, D., Cramer, C. & Eckert, H. *Chem. Mater.*, 2007, 19, 3162
- ¹⁶ Carta, D., Qiu, D., Guerry, P., Ahmed, I., Abou Neel, E. A., Knowles, J. C., Smith, M. E. & Newport, R. J. *J. Non-Cryst. Solids*, 2008, 354, 3671.

-
- ¹⁷ Michaelis V.K., Kachhadia, P., Kroeker, S. *Phys. Chem. Glasses: Eur. J. Glass Sci. Technol. B*, 2013, 54 (1), 20-26
- ¹⁸ Zeyer-Dusterer, M., Montagne, L., Palavit, G. & Jäger, C. *Solid State Nucl. Magn.*, 2005, 27, 50
- ¹⁹ L Koudelka et al 2009 IOP Conf. Ser.: Mater. Sci. Eng. 2 012015
- ²⁰ Lu, X., Lafon, O., Trébosc, J., Tricot, G., Delevoeye, L., Méar, F., Montagne, L., Amoureux, J.P. J. *Chem. Phys.* 2012, 137, 144201.
- ²¹ Feike, M., Jäger, C., Spiess, H.W. *J. Non-Cryst. Solids.*, 1998, 223, 200.
- ²² Jäger, C., Hartmann, P., Witter, R., Braun, M. *J. Non-Cryst. Solids* 2000, 263-264, 61.
- ²³ Ren, J., Eckert, H., *J. Chem. Phys.* 2013, 138, 164201.
- ²⁴ Garbow, J., Guillion, T., *J. Magn. Reson.* 1991, 95, 442.
- ²⁵ Bertmer, M., Eckert, H., *Solid State Nucl. Magn. Reson.* 1991, 95, 442.
- ²⁶ Elbers, S.; Strojek, W.; Koudelka, L.; Eckert, H. *Solid State Nucl. Magn. Reson.* 2005, 27, 65.
- ²⁷ Harris, R., Becker, E. *J. Magn. Reson.* 2002, 156(2), 323.
- ²⁸ Moudrakovski, I.L., *Ann. Rep. NMR Spec.*, 2013, 79, 129
- ²⁹ Burgess, K., Xu, Y., Leclerc, M.C., Bryce, D.L. *Inorg. Chem.* 2014, 53(1), 552.
- ³⁰ Faucher, A., Terskikh, V.V., Ye, E., Bernard, G.M., Wasylishen, R.E., *J. Phys. Chem. A*, 2015, 119 (49), 11847.
- ³¹ Millot, Y., Man, P. P., *Solid State Nucl. Magn. Reson.* 2002, 21, 21-43
- ³² Amoureux, J. P., Steuernagel, S., *J. Magn. Reson. A*, 1996, 123, 116-118
- ³³ Skibsted, J., Nielsen, N.C., Bildsøe, H. and Jakobsen, H.J., *J. Magn. Reson.*, 1991, 95(1), 88-117
- ³⁴ Massiot, D., Bessada, C., Coutures, J. P. & Taulelle, F. *J. Magn. Reson.*, 1990, 90, 231.

-
- ³⁵ Shelby, J.E., Introduction to Glass Science and Technology: Edition 2, 2005.
- ³⁶ Zielniok, D., Cramer, C., Eckert, H., *Chem. Mater.*, 2007, 19 (13), p. 3162-3170
- ³⁷ Janssen, M., Eckert, H., *Solid State Ionics*, 2000, 1007, p. 136-137
- ³⁸ Kroeker, S. & Stebbins, J. F. *Inorg. Chem.*, 2001, 40, 6239.
- ³⁹ Massiot, D., Bessada, C., Coutures, J. P. & Taulelle, F. J. *Magn. Reson.*, 1990, 90, 231.
- ⁴⁰ E. Ratai, M. Janssen, J.D. Epping, H. Eckert, *Phys. Chem. Glasses* 44 (2003) 45.
- ⁴¹ S. Kroeker, P.M. Aguiar, A. Cerquiera, J. Okoro, W. Clarida, J. Doerr, M. Olesiuk, G. Ongie, M. Affatigato, S.A. Feller, *Phys. Chem. Glasses: Eur. J. Glass Sci. Technol. Part B* 47 (2006) 393.
- ⁴² S. Kroeker, S.A. Feller, M. Affatigato, C.P. O'Brien, W.J. Clarida, M. Kodama, *Phys. Chem. Glasses* 44 (2003) 54.
- ⁴³ Aguiar, P. and Kroeker, S., (2007), *J. Non-cryst. Solids*, 353. 1834-1839.
- ⁴⁴ Ren, J., Eckert, H., *J. Phys. Chem. C*. 2012, 116 (23), p. 12747-12763
- ⁴⁵ Schulze, G. E. *R. Z. Phys. Chem.*, 1934, 24, 215.
- ⁴⁶ Grimmer, A.R., Müller, D., Gözel, G. and Kniep, R. *J. Anal. Chem.*, 1997, 357, p. 485-488
- ⁴⁷ Turner, G. L., Smith, K. A., Kirkpatrick, R. J., Oldfield, E. *J. Magnetic Resonance*, 1986, 67, 544-550
- ⁴⁸ Turner, G. L., Smith, K. A., Kirkpatrick, R. J., Oldfield, E. *J. Magnetic Resonance*, 1986, 70, 408-415
- ⁴⁹ Villa, M., Carduner, K.R., Chiodelli, G., *J. Solid State Chem.* 1987, 69, p. 19-23
- ⁵⁰ Morin, E. I., Wu, J., Stebbins, J. F. *Appl. Phys. A*, 2014, 116, p. 479-490